Cell Reports, Volume *9*

Supplemental Information

mTORC1 Controls PNS Myelination along the mTORC1-RXRγ-SREBP-Lipid Biosynthesis Axis in Schwann Cells

Camilla Norrmén, Gianluca Figlia, Frédéric Lebrun-Julien, Jorge A. Pereira, Martin Trötzmüller, Harald C. Köfeler, Ville Rantanen, Carsten Wessig, Anne-Lieke F. van Deijk, August B. Smit, Mark H.G. Verheijen, Markus A. Rüegg, Michael N. Hall, and Ueli Suter

Figure S1 - linked to Figure 1

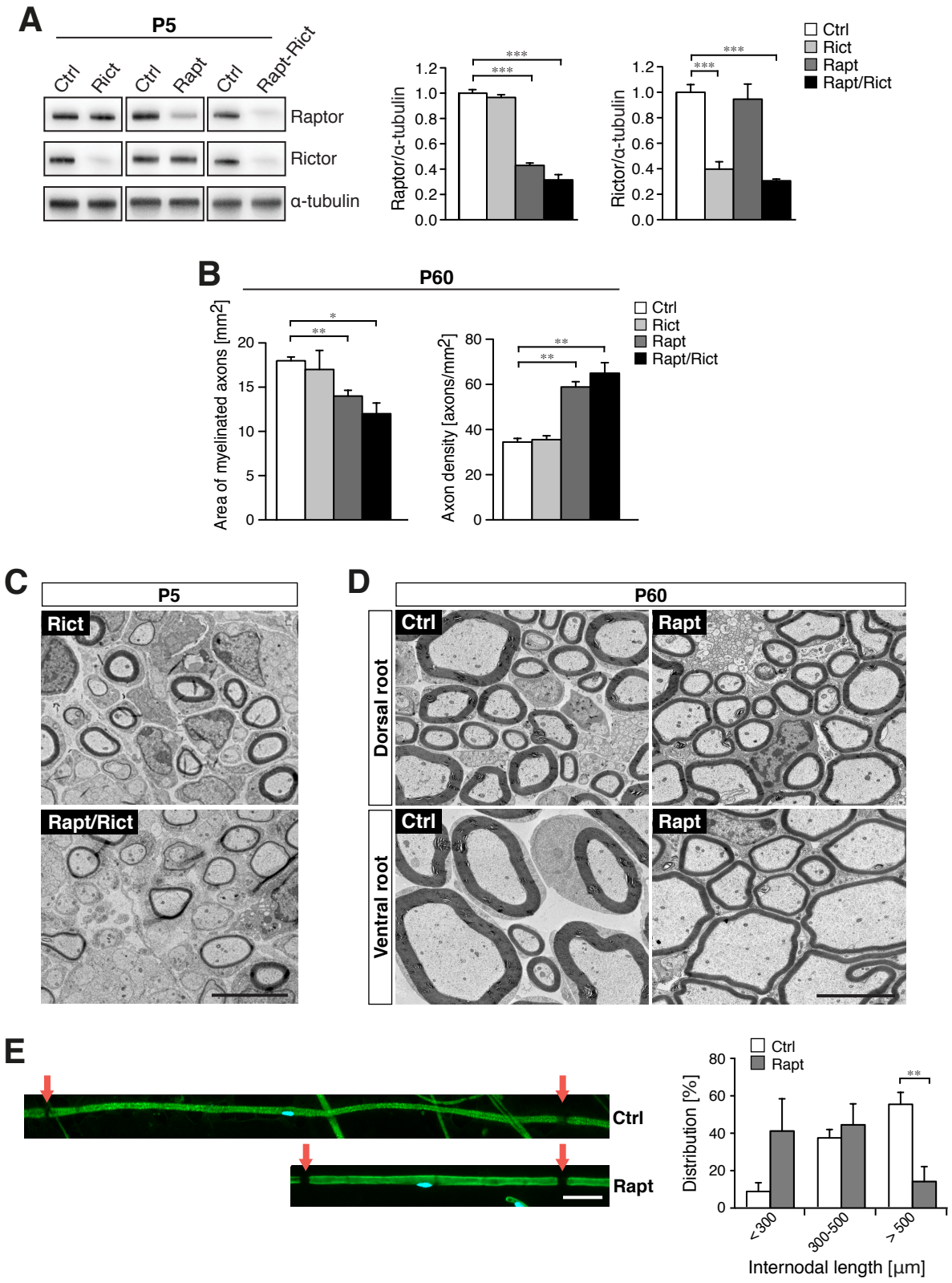

Figure S1. Hypomyelination in raptor mutant mice in proximal nerves fibers

(A) Western blotting analysis showing loss of raptor and rictor proteins in sciatic nerve lysates from control, rictor, raptor and raptor/rictor mutant mice at P5. Expression levels in at least 3 mice per genotype were quantified, and average levels are shown relative to levels from control mice. Error bars represent SEM. *** $P < 0.001$.

(B) Quantification of the area of myelinated axons and axon density of the main fascicle of sciatic nerves from control, rictor, raptor and raptor/rictor mutant mice at P60 (nerves depicted in Figure 1A). Results are shown as mean from 3 different mice per genotype. Error bars represent SEM. * $P < 0.05$, ** $P < 0.01$.

(C) Electron microscopy (EM) micrographs of ultrathin cross sections of sciatic nerves from rictor and raptor/rictor mutant mice at P5. Compare with control and raptor mutant mice shown in Figure 1C. Scale bar: 5 μm.

(D) EM micrographs of ultrathin cross sections of dorsal and ventral L5 roots from control and raptor mutant mice at P60, showing hypomyelination in raptor mutants in both sensory (dorsal root) and motor fibers (ventral root). Scale bar: 5 μm.

(E) Analysis of teased sciatic nerve fibers from control and raptor mutants (2-7 months old, *N*=4 mice per genotype) stained for MBP (green) shows increased percentage of short internodes (< 300 μm) and significantly fewer long internodes (> 500 μm) in raptor mutants compared to control mice. Red arrows: Nodes of Ranvier.

Figure S2 - linked to Figure 2

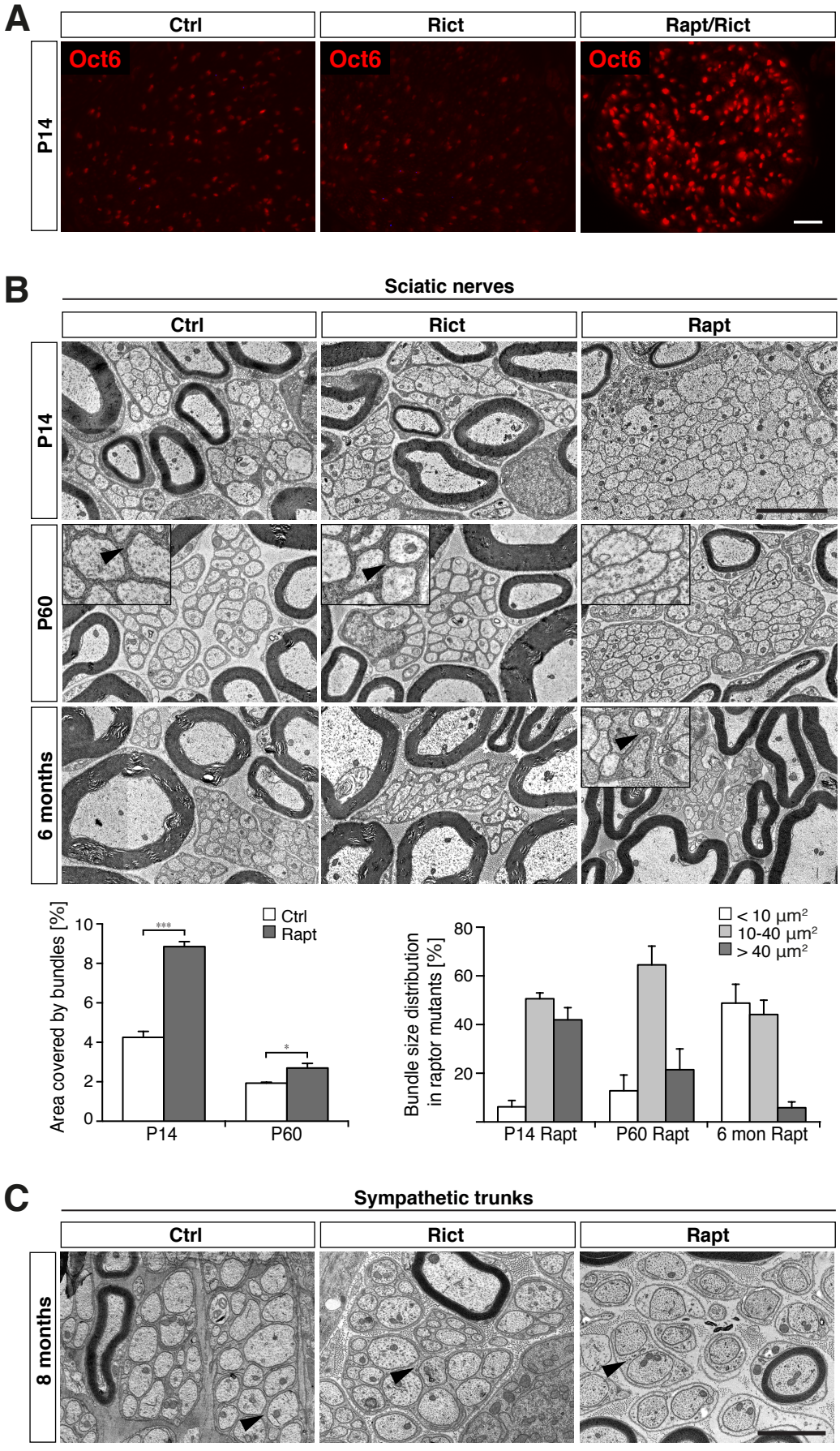

Figure S2. Radial sorting defect in raptor mutant mice

(A) Oct6 immunostaining of transverse cryosections from control, rictor and raptor/rictor mutant sciatic nerves at P14, showing persistent Oct6 expression in raptor/rictor mutants at P14. Compare with raptor mutant mice shown in Figure 2B. Scale bar: 50 μm.

(B) EM micrographs of ultrathin cross sections of sciatic nerves from control, rictor and raptor mutant mice at P14, P60 and 6 months, showing large, immature unsorted bundles in raptor mutants at P14 and P60, whereas control and rictor mutants display normal mature Remak bundles. The high magnification inserts illustrate that the bundles in raptor mutant mice lack Schwann cell cytoplasm between axons still at P60, whereas some cytoplasm can be found in raptor mutants in 6 month-old nerves. Black arrowheads: Schwann cell cytoplasm. Scale bar: 2 μm. The nerve area covered by bundles was quantified in control and raptor mutant nerves. The data show that significantly larger areas are covered with bundles in raptor mutants. The sizes of the individual bundles were also quantified in raptor mutants, and show a decrease in size with age. *N*=3 mice for each genotype. Error bars represent SEM. * $P < 0.05$, *** $P < 0.001$.

(C) EM micrographs of ultrathin cross sections of sympathetic trunks (enriched in small caliber axons and Remak bundles) from control, rictor and raptor mutant mice at 8 months, showing Remak bundle-like structures with Schwann cell cytoplasm also in raptor mutants. Black arrowsheads: Schwann cell cytoplasm. Scale bar: 2 μm.

Figure S3 - linked to Figure 3

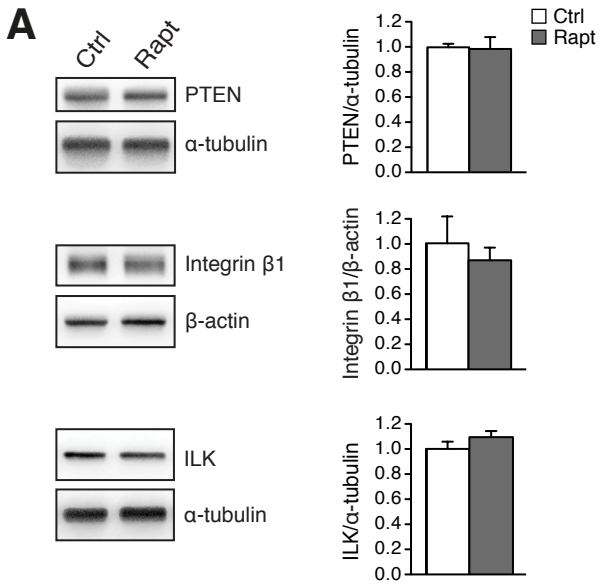

Figure S3. mTORC1 deficiency in Schwann cells does not affect common factors regulating myelination

(A) Western blotting analysis showing no change in expression of the indicated proteins in sciatic nerve lysates from control and raptor mutant mice at P5. Expression levels in at least 3 mice per genotype were quantified, and average levels are shown relative to levels from control mice. Error bars represent SEM.

Figure S4 - linked to Figure 5

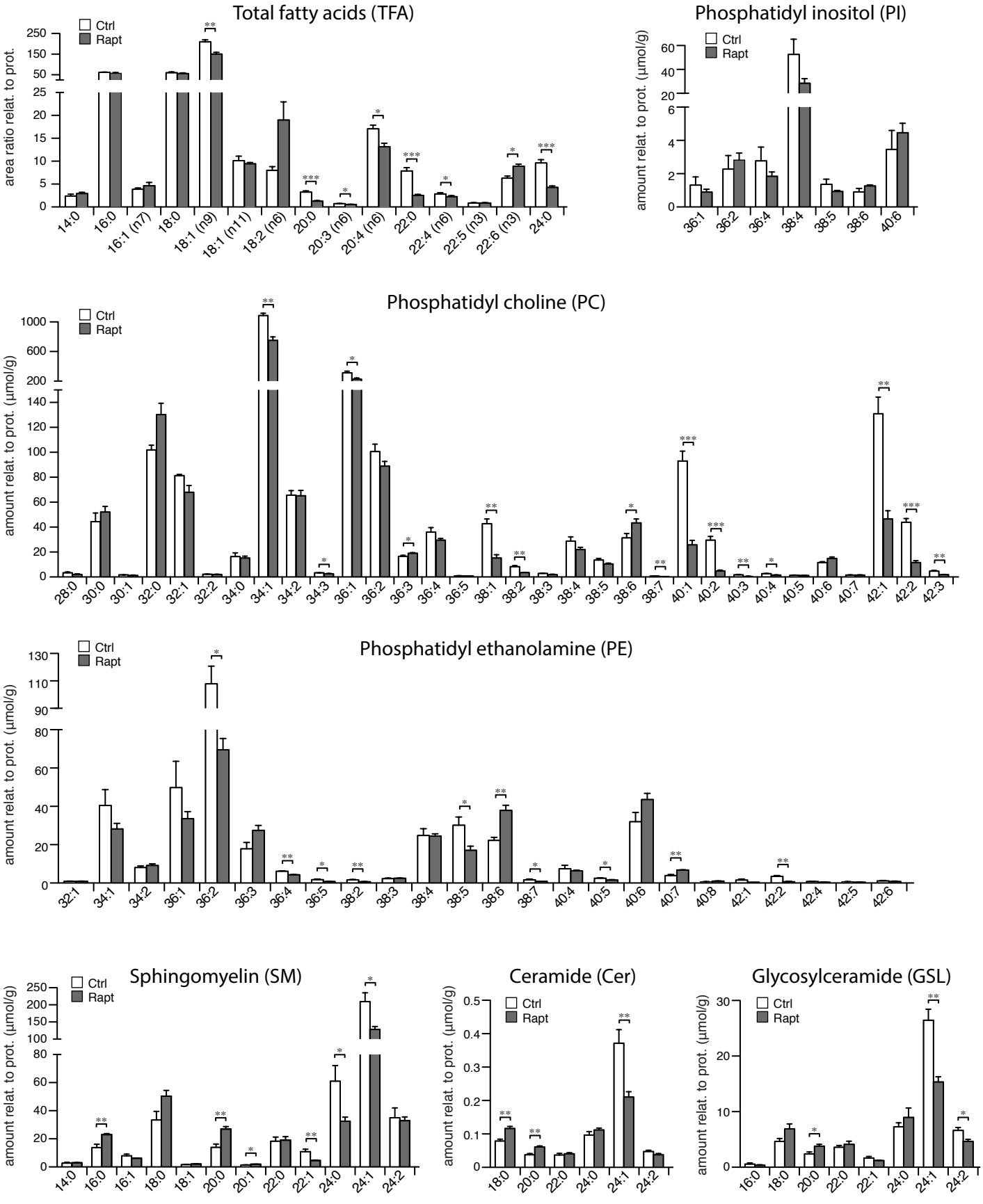

Figure S4. Lipid profile of sciatic nerves of control and raptor mutant mice

Lipid extracts of P60 sciatic nerves from control and raptor mutant mice were analyzed using liquid chromatography-mass spectrometry (LC-MS). Depicted are individual fatty acids (FA) as well as individual phosphatidylcholines (PC), phosphatidylethanolamines (PE), phosphatidylinositols (PI), sphingomyelin (SM), ceramides (CER) and glycosylceramides (GSL). *N*=3 for control mice, *N*=4 for raptor mutant mice, error bars represent SEM. * $P < 0.05$, ** $P < 0.01$, *** $P < 0.001$.

Figure S5 - linked to Figure 7

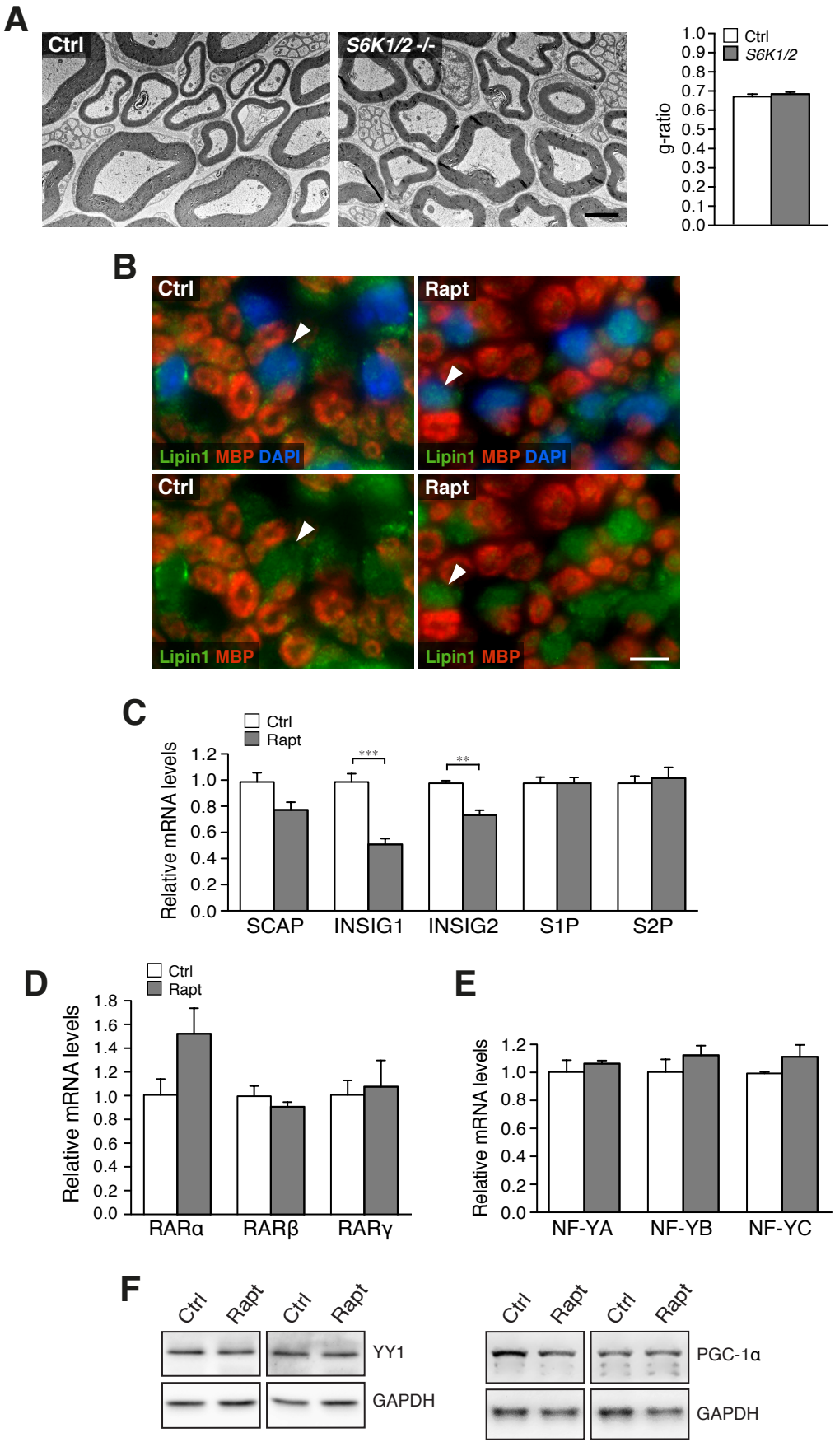

Figure S5. Analysis of factors linked to SREBP signaling

(A) EM micrographs of ultrathin cross sections of sciatic nerves from control and *S6K1/2* knockout mice at P60, showing no difference in myelin thickness. Myelin thickness was quantified as g-ratio. Scale bar: 2 μm.

(B) Immunostaining for lipin1 (green) and MBP (red) in transverse cryosections from control and raptor mutant sciatic nerves at P14, showing no major difference in lipin1 localization. Arrowheads indicate examples of nuclei. Scale bar: 5 μm.

(C) qRT-PCR analysis of expression of genes linked to SREBP processing in sciatic nerve lysates from control and raptor mutant mice at P8, showing no significant changes in SCAP, S1P and S2P expression, and a decrease in INSIG1 and INSIG2. *N*=4 mice for each genotype, error bars represent SEM. ** $P < 0.01$, *** $P < 0.001$.

(D,E) qRT-PCR analysis of gene expression of nuclear receptors of the retinoic acid receptor (RAR) family, and of the NF-Y family of transcription factors in sciatic nerve lysates from control and raptor mutant mice at P8, showing no significant changes (although RARα shows a tendency for increase). N=4 mice for each genotype, error bars represent SEM.

(F) Western blotting analysis of indicated proteins in sciatic nerve lysates from control and raptor mutant mice at P5, showing equal expression of YY1 and PGC-1α in two mice of each genotype.

Figure S6 - linked to Figure 7

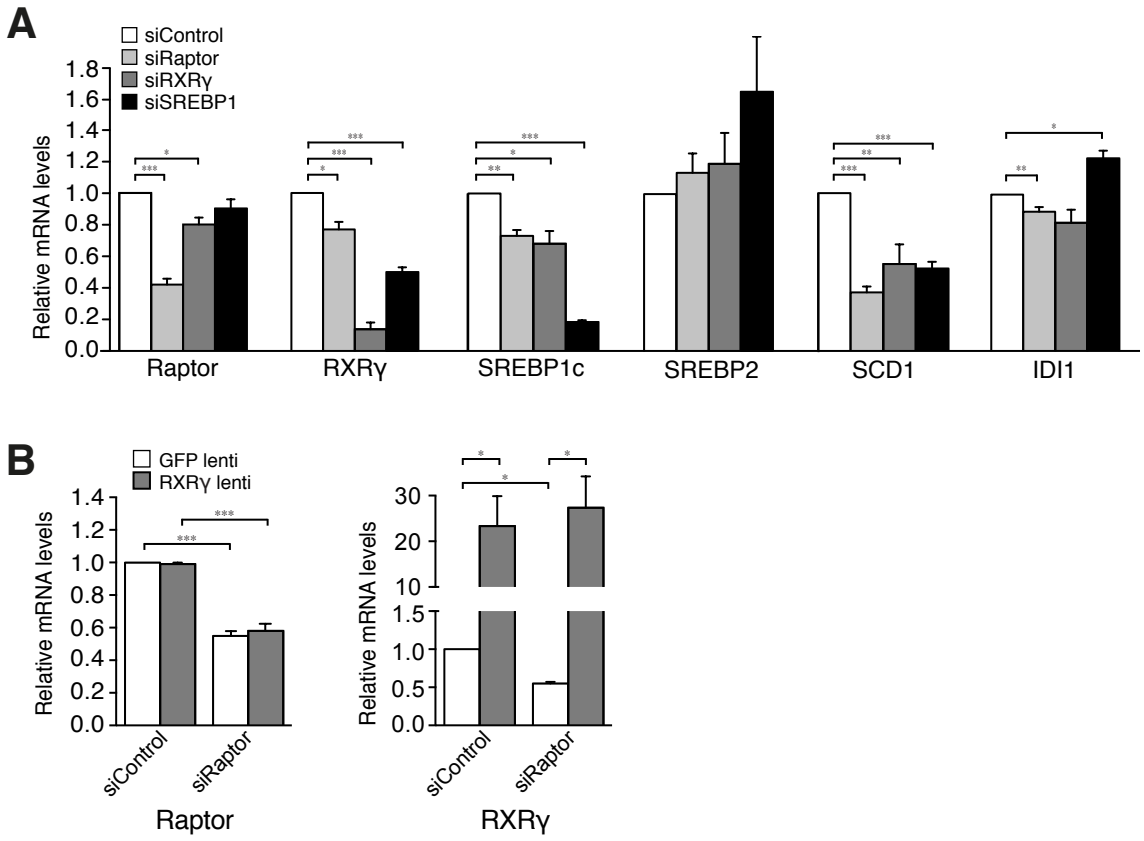

Figure S6. RXRγ regulates *Srebf1c* downstream of mTORC1

(A) Primary rat Schwann cells were transfected with a pool of 2 siRNAs targeting Raptor, RXRγ or SREBP1, or a non-targeting siRNA (siControl). Expression of the indicated genes was analyzed by qRT-PCR at 72 hours after transfection. The results are shown as mean ratio of siControl levels from 3 independent experiments. Error bars represent SEM. * P < 0.05, ** P < 0.01, *** P < 0.001. The results are similar to those shown in Figure 7D of the main text, but using a different set of siRNAs.

(B) Primary rat Schwann cells were first transfected with a pool of siRNAs against raptor, and 5 hours later transduced with a lentivirus expressing RXRγ or a GFP-expressing control virus. Expression of raptor and RXRγ was analyzed 72 hours later by qRT-PCR. Results are shown as mean ratio versus control virus levels from 3 independent experiments, and indicate successful downregulation of raptor and successful upregulation of RXRγ. Error bars represent SEM. * P < 0.05, *** P < 0.001. See Figure 7G for qRT-PCR of other genes in this experiment.

Supplemental Experimental Procedures

Western blotting

For Western blotting, sciatic nerves were stripped from the epineurium, and lysed in RIPA lysis buffer (50 mM Tris-HCl, 1% NP-40, 0.25% Na-deoxycholate, 150 mM NaCl), SDS lysis buffer (25 mM Tris-HCl, 95 mM NaCl, 10 mM EDTA, 2 % SDS) or urea lysis buffer (8 M urea, 10 mM Tris-HCl, 150 mM NaCl, 5 mM EDTA, 1% Triton X-100), supplemented with protease and phosphatase inhibitors (Roche). Proteins were separated using precast Mini-PROTEAN TGX gels (Biorad) and standard SDS-PAGE and Western blotting procedures. The following antibodies were used: P-Akt (S473), P-Akt (T308), Akt, P-4-EBP (S65), 4E-BP1, P-ERK1/2 (T202/Y204), ERK1/2, P-p70 S6K (T389), p70 S6K, SCD1, PTEN, Raptor and Rictor (all from Cell Signaling Technology); P-ErbB2 (Y1248) and ErbB2 (Abcam); MBP (Serotec); MAG (Invitrogen); P0 (Astex); Krox20 (Covance); Oct6 (kind gift from Dies Meijer, University of Edinburgh, Scotland); Sox10 (R&D Systems); RXRγ (Abcam); ILK (BD Biosciences); Integrin β1 (Abcam); SREBP1 and YY1 (Santa Cruz Biotechnology); SREBP2 (Camargo et al., 2012); FASN (Abcam); PGC-1 (Millipore), IDI1 and HMGCR (kind gifts from Werner Kovacs, ETH Zürich, Zurich, Switzerland); α-tubulin (Sigma); GAPDH (HyTest) and β-actin (Sigma). Secondary antibodies were obtained from Promega. Signals were detected using the chemiluminescence imaging system FUSION Fx7 (Vilber Lourmat), and bands were quantified using Quantity One software (Biorad).

qRT-PCR

Total RNA from sciatic nerves (stripped from the epineurium) or rat Schwann cells was extracted using Qiazol lysis reagent (Qiagen), and cDNA was produced by Superscript III Reverse Transcriptase (Invitrogen) or Maxima Reverse Transcriptase (Thermo Scientific). qRT-PCR analysis was performed on a Light Cycler 480 II (Roche), using LightCycler SYBR Green I Master Mix (Roche). Relative expression values for each gene were obtained by normalizing to β-actin expression (and further confirmed relative to GAPDH expression), and differences between samples were calculated using the $2^{-\Delta\Delta Ct}$ method. Primer sequences are listed in Table S1.

Nerve histology and morphometry

Processing of mouse tissue for histological analysis by light and electron microscopy was performed as previously described (Pereira et al., 2010). Toluidine blue-stained semithin sections (0.6 μm) of transverse nerves were imaged using a light microscope (Carl Zeiss Axioplan 2), and complete nerve cross sections were reconstructed from multiple images using

Adobe Photoshop CS5 software. For quantification of myelinated axons and their diameters, the images were analyzed in a pipeline created in the Anduril analysis framework as described (Rantanen et al., 2014). After manual inspection and correction, the area and diameter of each object was measured. The ratio of the axon diameter/fiber diameter (g-ratio) was measured using Adobe Photoshop CS5 software. For electron microscopy, ultrathin sections were collected on carbon-coated Formvar grids (Electron Microscopy Sciences) and analyzed using a Morgagni 268 transmission electron microscope.

Immunohistochemistry

For cryosections, sciatic nerves were fixed with 4% paraformaldehyde (PFA), dehydrated in 30% sucrose, and embedded in OCT (Tissue Tek). Teased fibers were prepared fresh on TESPA-coated slides. Cryosections (8 µm) or teased fibers were permeabilized/fixed with methanol/PFA, blocked for 1 hour at RT in blocking buffer (0.1% Triton X-100, 10% goat serum and 1% BSA in PBS), and incubated with primary antibodies overnight at 4°C in blocking buffer. The following antibodies were used: Oct6 (kind gift from Dies Meijer, University of Edinburgh, Scotland), MBP (Serotec), FASN (Abcam), S100 (DAKO) and lipin1 (Peterson et al., 2011) (a kind gift from Thurl E. Harris, University of Virginia, USA). Alexa 488 and Cy3 fluorochrome-conjugated secondary antibodies were used for signal detection. Samples were mounted with DAPI-containing Vectashield (Vector Laboratories), and analyzed using an epifluorescent microscope (Axioplan 2, Carl Zeiss), equipped with a CCD camera (AxioCam MRm, Carl Zeiss). Images were acquired with Axio Vision 4.6 acquisition software (Carl Zeiss), and further processed using Photoshop CS5 (Adobe).

Lipid analysis

For lipid profiling, sciatic nerves from P60 mice were stripped from the epineurium, and lipid extraction was performed as previously described (Matyash et al., 2008). Lipid extracts were analyzed using mass spectrometry according to published methods (Fauland et al., 2011). In brief, lipid species were subjected to internal standardization and data acquisition by HPLC coupled to an FT-ICR-MS hybrid mass spectrometer (LTQ-FT, Thermo Scientific), and data was processed using Lipid Data Analyzer software as previously described (Hartler et al., 2011). Fatty acids were detected using GC-MS (Trace-DSQ, Thermo Scientific). Chemicals used for the lipid analysis were from Merck KGaA or Sigma-Aldrich. Lipid standards (Supplemental Table S2) were obtained from Avanti Polar Lipids Inc.

Processing of Lipid Extracts for Lipid Species Analysis. Lipid extracts were evaporated and resuspended in chloroform/methanol (1/1; v/v), and each extract was then split for analysis of total fatty acids, free fatty acids, positive ESI LC-MS/MS and negative ESI LC-MS/MS. Lipid

extracts for LC-MS/MS analysis were evaporated, spiked with a set of 26 internal standards (supplemental table S2) and again resuspended in chloroform/methanol (1/1; v/v).

Gas Chromatography with Electron Impact Mass Spectrometry (GC-EI/MS) of total fatty acids (free + esterified). Aliquots of lipid extracts were dried and suspended in methanolic NaOH. After heat incubation, BF_3 was added and samples were again incubated at 80°C. Fatty acid methyl esters were extracted with saturated NaCl and hexane. The hexane phase was dried and methyl esters dissolved in hexane. A Trace-DSQ GC-MS (Thermo Scientific) equipped with a TR-FAME 30m column was used for analysis in split mode, with helium as carrier gas and 250°C injector temperature. The mass spectrometer was run in electron impact (EI) mode and fatty acids were detected in full scans of m/z 80 - 400. Source temperature was set to 250°C and the transfer line temperature to 200°C.

Supplemental Tables

Table S1. qRT-PCR primers

Target	Forward primer	Reverse primer
MOUSE		
Srebp1c	5'-GCCATGGATTGCACATTTGA-3'	5'-TGGTTGTTGATGAGCTGGAGC-3'
Srebp1a	5'-GAACAGACACTGGCCGAGATGT-3'	5'-GGTTGTTGATGAGCTGGAGCAT-3'
Srebp2	5'-GCGTTCTGGAGACCATGGA-3'	5'-ACAAAGTTGCTCTGAAAACAAATCA-3'
FASN	5'-GTTGGCCCAGAACTCCTGTA -3'	5'-GTCGTCTGCCTCCAGAGC -3'
SCD1	5'-CAGCCGAGCCTTGTAAGTTC-3'	5'-GCTCTACACCTGCCTCTTCG-3'
HMGCR	5'-GGCCTCCATTGAGATCCG-3'	5`-CACAATAACTTCCCAGGGGT-3
IDI1	5'-TCAACTTCATGTTCACCCCA-3'	5'-GAGTTGGGAATACCCTTGGA-3'
SCAP	5'-CTGCTACCCGCTGCTGAA-3'	5'-AGAATTCCACAGGTCCCGTTC-3'
INSIG1	5'-TCGTTGGCATCAACCACGCCA-3'	5'-GCCGCTTCGGGAACGATCA-3'
INSIG2	5'-GTCCAGTGTCATGCGCTGCGT-3'	5'-CAGTGCAGCCAGTGTGAGGGA-3'
S1P	5'-GGTGCTGGAGTGCGGGGTTC-3'	5'-ACCCCAGGAAGTCTCCGGGC-3'
S2P	5'-TCACCAGTCCAGCAGCTAAGGA-3'	5'-GCCTCTGGGTCCAATGGCAGG-3'
LXRα	5'-GCCCTGCACGCCTACGT-3'	5'-TAGCATCCGTGGGAACATCA-3'
LXRβ	5'-GCTGATGATCCAGCAGTTAG-3'	5'-CGGAGAAAGATCGTTTGTTG-3'
RXRα	5'-GTTGGAGAGTTGAGGGACGA-3'	5'-GGGCATGAGTTAGTCGCAGA-3'
RXRβ	5'-GTCCACAGGCATCTCCTCAG-3'	5'-ACTGGCATGAAAAGGGAGG-3'
RXRγ	5'-CAAGGCTACTGAAGGGCTCA-3'	5'-GCAGCCAACATGTATGGAAA-3'
RARα	5'-GGGAGGGCTGGGTACTATCT-3'	5'-AGCACCAGCTTCCAGTCAGT-3'
RARβ	5'-CTCTGTGCATTCCTGCTTTG-3'	5'-AAGTGCTTTGAAGTGGGCAT-3'
RARγ	5`-CGAGCTGGTGCTCTGTGTC-3	5'-ACCATTTGAGATGCTGAGCC-3'
NF-YA	5'-CTCTACAGATCCCAGGCAGC-3'	5'-GTTTCGGGGTCCGGTACT-3'
NF-YB	5'-TAGCTGGGAGGCATCTGTG-3'	5'-AGGATCCACCACCTTTTTGA-3'
NF-YC	5`-AGAAGGACTGGAGGCTTTGC-3	5'-GCTGCTTTCTTCGCTGGAC -3'
β-actin	5'-TTCTTTGCAGCTCCTTCGTT-3'	5'-ATGGAGGGGAATACAGCCC-3'
GAPDH	5'-TGGTGAAGGTCGGTGTGAAC-3'	5'-TTCCCATTCTCGGCCTTGAC-3'
RAT		
Raptor	5`-CCTTGGTCCTGTGCCTGAAT-3	5'-CAAGGCTCTGCTTGTACCGA-3'
RXRγ	5`-ATGAAGTTTCCCACCGGCTT-3	5'-ATGACTGTCCATCGGCTTCC-3'
Srebp1c	5'-GCCATGGATTGCACATTTGA-3'	5'-TGGTTGTTGATGAGCTGGAGC-3'
Srebp1a	5'-GAACAGACACTGGCCGAGATGT-3'	5'-GGTTGTTGATGAGCTGGAGCAT-3'
Srebp2	5'-GCGTTCTGGAGACCATGGA-3'	5'-ACAAAGTTGCTCTGAAAACAAATCA-3'
SCD1	5'-CAGCCGAGCCTTGTAAGTTC-3'	5'-GCTCTACACCTGCCTCTTCG-3'
FASN	5`-TGCCTAAGCGGTCTGGAAAG-3	5'-TTTGTTCCTCGGAGTGAGGC-3'
IDI1	5`-GATGCCATGGGTGTCAAACG-3	5'-TGGGATCCGGATTCAGGGTT-3'
β-actin	5'-ACAACCTTCTTGCAGCTCCTC-3'	5'-GACCCATACCCACCATCACAC-3'

Table S2. List of internal standards used in LC-MS (lipid analysis)

Product number	Shorthand nomenclature	Amount/sample [pmol]
LM-1100	PE 12:0/13:0	160
LM-1102	PE 17:0/20:4	160
LM-1103	PE 21:0/22:6	160
LM-1104	PE 17:0/14:1	160
LM-1302	PS 17:0/20:4	240
LM-1300	PS 12:0/13:0	240
LM-1304	PS 17:0/14:1	240
LM-1000	PC 12:0/13:0	200
LM-1002	PC 17:0/20:4	200
LM-1003	PC 21:0/22:6	200
LM-1004	PC 17:0/14:1	200
LM-1601	LPC 17:1	80
LM-4100	Cholesterol (D7)	6400
LM-6002	Sphingolipid mix I	120
LM-1500	PI 12:0/13:0	320
LM-1502	PI 17:0/20:4	320
LM-1504	PI 17:0/14:1	320

Supplemental References

Camargo, N., Brouwers, J.F., Loos, M., Gutmann, D.H., Smit, A.B., and Verheijen, M.H. (2012). High-fat diet ameliorates neurological deficits caused by defective astrocyte lipid metabolism. Faseb J *26*, 4302-4315.

Fauland, A., Kofeler, H., Trotzmuller, M., Knopf, A., Hartler, J., Eberl, A., Chitraju, C., Lankmayr, E., and Spener, F. (2011). A comprehensive method for lipid profiling by liquid chromatography-ion cyclotron resonance mass spectrometry. J Lipid Res *52*, 2314-2322.

Hartler, J., Trotzmuller, M., Chitraju, C., Spener, F., Kofeler, H.C., and Thallinger, G.G. (2011). Lipid Data Analyzer: unattended identification and quantitation of lipids in LC-MS data. Bioinformatics *27*, 572-577.

Matyash, V., Liebisch, G., Kurzchalia, T.V., Shevchenko, A., and Schwudke, D. (2008). Lipid extraction by methyl-tert-butyl ether for high-throughput lipidomics. J Lipid Res *49*, 1137-1146.

Pereira, J.A., Baumann, R., Norrmen, C., Somandin, C., Miehe, M., Jacob, C., Luhmann, T., Hall-Bozic, H., Mantei, N., Meijer, D*., et al.* (2010). Dicer in Schwann Cells Is Required for Myelination and Axonal Integrity. J Neurosci *30*, 6763-6775.

Peterson, T.R., Sengupta, S.S., Harris, T.E., Carmack, A.E., Kang, S.A., Balderas, E., Guertin, D.A., Madden, K.L., Carpenter, A.E., Finck, B.N*., et al.* (2011). mTOR Complex 1 Regulates Lipin 1 Localization to Control the SREBP Pathway. Cell *146*, 408-420.

Rantanen, V., Valori, M., and Hautaniemi, S. (2014). Anima: Modular workflow system for comprehensive image data analysis. Front Bioeng Biotechnol *2*.